

Supporting Information

Hydrophobic Collapse-Driven Nanoparticle Coating with Poly- Adenine Adhesives

Dan Zhu,^a Jiang Li,^{b,c} Lianhui Wang,^a Qian Li,^c Lihua Wang,^b Bo Song,^{d*} Ruhong Zhou^{e*} and
Chunhai Fan^{c*}

^a Key Laboratory for Organic Electronics and Information Displays & Jiangsu Key Laboratory for Biosensors, Institute of Advanced Materials (IAM), Jiangsu National Synergetic Innovation Center for Advanced Materials (SICAM), Nanjing University of Posts and Telecommunications, Nanjing 210023, China

^b The Interdisciplinary Research Center, Shanghai Synchrotron Radiation Facility, Zhangjiang Laboratory, Shanghai Advanced Research Institute, Chinese Academy of Sciences, Shanghai 201210, China

^c School of Chemistry and Chemical Engineering, Frontiers Science Center for Transformative Molecules and National Center for Translational Medicine, Shanghai Jiao Tong University, Shanghai 200240, China

^d School of Optical-Electrical Computer Engineering, University of Shanghai for Science and Technology, Shanghai 200093, China

^e Institute of Quantitative Biology, College of Life Sciences, Zhejiang University, Hangzhou 310058, China

* Corresponding authors

E-mail addresses: bsong@usst.edu.cn; rhzhou@zju.edu.cn; fanchunhai@sjtu.edu.cn

Table of contents:

Experimental Section-----	S3
Table S1. Oligonucleotide sequences-----	S7
Figure S1. A typical structure at the initial time of the MD simulation-----	S8
Figure S2. Trajectories of the contact area per base (CApB) for the A ₇ sequence adsorbing on the gold surface-----	S9
Figure S3. Trajectories of CApB for the A ₃ T ₃ A ₃ sequence adsorbing on the gold surface-----	
-----	S10
Figure S4. Trajectories of CApB for the A ₃ T ₂ A ₃ sequence adsorbing on the gold surface-----	
-----	S11
Figure S5. Trajectories of CApB for the A ₃ T ₃ A ₃ sequence adsorbing on the gold surface-----	
-----	S12
Figure S6. Trajectories of CApB for the A ₃ T ₄ A ₃ sequence adsorbing on the gold surface-----	
-----	S13
Figure S7. Trajectories of CApB for the A ₃ T ₅ A ₃ sequence adsorbing on the gold surface-----	
-----	S14
Figure S8. Trajectories of CApB for the (AT) ₅ A sequence adsorbing on the gold surface-----	
-----	S15
Figure S9. Trajectories of CApB for the T ₁₁ sequence adsorbing on the gold surface---	
-----	S16
Reference-----	S17

Experimental Section

Chemicals and Materials.

All the DNA samples listed in Table S1 were synthesized and purified by Takara Biotechnology Co. (Dalian, China). NaCl, Na₂HPO₄ and NaH₂PO₄ were obtained from China National Pharmaceutical Group Corporation (Shanghai, China). Mercaptoethanol (ME) was purchased from Sigma-Aldrich Company Ltd. (USA). AuNPs (5 nm, 10 nm, 20 nm, 30 nm and 50 nm in diameter) were purchased from Ted Pella (Redding, CA).

Apparatus.

Fluorescence measurements were performed on F4500 (Hitachi, Japan). Absorbance experiments of AuNPs and DNA was performed on U3900 (Hitachi, Japan).

DNA adsorption measurements.

The DNA adsorption processes on AuNP were monitored by using fluorescence quenching method according to the literature^{1,2}. In detail, dilutions of series of FAM-labeled DNA in 20 mM PBS (20 mM PB, 20 mM NaCl, pH 7.4) were prepared and placed in a 96-well plate. The low concentration of salt buffer was set to avoid the aggregation of AuNPs. Fluorescence kinetic measurements (ex, 485 nm; em, 530 nm) were started after the same volume of AuNP solution was added at room temperature. The final concentration of AuNP and DNA was 8 nM and 40 nM, respectively.

Preparation of Diblock Oligonucleotide-Modified Gold Nanoparticles

The prepared AuNPs were first incubated with Diblock Oligonucleotide in a rational ratio according to the size of AuNPs (for 5 nm-10 nm AuNPs, [DNA]: [AuNP] = 200:1; for 20 nm AuNPs, [DNA]: [AuNP] = 300:1; for 30 nm AuNPs, [DNA]: [AuNP] = 1000:1; for 50 nm AuNPs, [DNA]: [AuNP] = 3000:1) for 16 h, 1M sodium phosphate buffer (1 M NaCl, 100 mM PB, pH 7.4) was added to the mixture for 5 times to reach a final concentration of 0.1 M PBS. The salting process was allowed by incubation for another 40 h at room temperature. Then, the mixture was washed 3 times with 0.1 M sodium phosphate buffer (0.1 M NaCl, 10 mM PB, pH 7.4) through centrifugation (For 5-10 nm AuNPs, 15000 rpm, 20 min; for 20 nm AuNPs, 12000

rpm, 20 min; for large AuNPs, the rotational speed should be slower and the time of centrifugation should be shorter to avoid the aggregation of AuNPs) to remove excess DNA. Then, the supernatant was removed and the nanoparticles were resuspended in 0.1M PBS (pH 7.4).

Quantification of Diblock-Oligonucleotide loaded on AuNPs

The concentration of AuNPs and the FAM-labeled diblock DNA in each sample were measured to quantify the number of DNA attached to each AuNP. The concentrations of AuNPs were determined by UV-visible spectroscopy measurements and the absorbance values were related to the concentration of nanoparticles via Beer's law. The extinction coefficient (ϵ) and the absorbance maximums (λ_{\max}) for each particle size used in our research are as follows: for 5 nm AuNPs, $\epsilon = 1.10 \times 10^7 \text{ M}^{-1}\text{cm}^{-1}$, $\lambda_{\max} = 515\text{-}520 \text{ nm}$; for 10 nm AuNPs, $\epsilon = 1.01 \times 10^8 \text{ M}^{-1}\text{cm}^{-1}$, $\lambda_{\max} = 518 \text{ nm}$; for 20 nm AuNPs, $\epsilon = 9.21 \times 10^8 \text{ M}^{-1}\text{cm}^{-1}$, $\lambda_{\max} = 524 \text{ nm}$; for 30 nm AuNPs, $\epsilon = 3.36 \times 10^9 \text{ M}^{-1}\text{cm}^{-1}$, $\lambda_{\max} = 526 \text{ nm}$; for 50 nm AuNPs, $\epsilon = 1.72 \times 10^{10} \text{ M}^{-1}\text{cm}^{-1}$, $\lambda_{\max} = 535 \text{ nm}$.

To determine the concentration of FAM-labeled DNA in each aliquot, the DNA was chemically displaced from the AuNPs' surface using ME³. The displacement was achieved by adding ME (with a final concentration of 20 mM in 0.3 M NaCl, 10 mM phosphate buffer solution (pH 7.4)) into the FAM-labeled DNA-AuNPs solution. The mixture was then incubated for 18 h with shaking at room temperature. The released DNA probes were then separated via centrifugation and the fluorescence was recorded by a fluorescence spectrometer. The fluorescence was converted to molar concentrations of probes by comparing to a standard linear calibration curve which was prepared with known concentrations of oligonucleotides with identical buffer pH, ionic strength and ME concentration. The number of oligonucleotides per AuNP was calculated by dividing the concentration of fluorescent oligonucleotides by the concentration of AuNPs. All experiments were repeated three times using fresh samples to obtain error bars.

MD simulation.

To obtain binding picture of the ssDNA specificity on the gold surface, we

performed MD simulations for the adsorption processes of the ssDNA sequence on an AuNP's Au(111) surface immersed in water. A periodic box of $6.0 \text{ nm} \times 6.0 \text{ nm} \times 6.0 \text{ nm}$ was utilized for the simulations. The ssDNA sequences, including A_7 , $A_3T_nA_3$ ($n = 1\sim 5$), $(AT)_5A$ and T_{11} (poly(T)) were employed in the simulations. The Improved DNA Force Field for ssDNA is used to model ssDNA⁴. In total, 1512 gold atoms were arranged in three layers to model the AuNP's Au(111) surface with an fcc lattice constant of $a = 4.078 \text{ \AA}$. The gold atoms were fixed to their starting position during the simulations. We employed the 12-6 Lennard-Jones potential to describe the interaction between the Au surface and the ssDNAs. The Au atoms were characterized as uncharged Lennard-Jones particles, with a radius of cross-section $\sigma_{\text{Au}} = 2.9 \times 10^{-1} \text{ nm}$ and a depth of the potential well $\epsilon_{\text{Au}} = 4.3 \times 10^{-1} \text{ kJ}\cdot\text{mol}^{-1}$, which are used in a very recent study. The SPCE water model was used for solvation. The negatively charged backbones of ssDNA are neutralized using Na^+ counter ions. The initial configuration for the hybrid systems is considered by keeping the ssDNA at about 10.0 \AA distance away from the gold surface (see Figure S1). The high energy contacts between the atoms in the initial conformations of the hybrid systems are removed by minimizing the energy of each system using steepest decent integration method. Following that, MD simulations are performed using leap-frog algorithm for integrating Newton's equation of motion for 200 ns at constant temperature (300 K). The velocity rescaling thermostat was applied for temperature coupling. The particle-mesh Ewald method with a real-space cutoff of 10 \AA was used to treat long-range electrostatic interactions, and a 12 \AA smooth cutoff was applied to all van der Waals interactions. In the simulations, the covalent bonds involving the H atoms were constrained by the LINCS algorithm. The time step for the simulations was set at 1 fs. All MD simulations were conducted using the Gromacs 4.5.4 package. The MD simulations of A_7 , $A_3T_nA_3$, $(AT)_5A$ and T_{11} adsorption on the Au(111) surface were performed and ten trajectories were obtained for each sequence. The results are presented in Figs. S2-S9.

A contact area per base (CApB) between the ssDNA and Au surface was

calculated to describe the adsorption strength between them, where the contact area was defined as a half of the difference between the solvent accessible surface area (SASA) of the ssDNA-Au complex and the sum of the SASAs of the ssDNA and the gold separately. In order to quantitatively better describe the adsorption affinity of the ssDNA sequence on the gold surface, we calculated the statistical average of the CApB areas based on the MD simulations using the following formula:

$$C\bar{A}pB = \frac{1}{N} \sum_{i=1}^N \frac{1}{t_2 - t_1} \cdot \int_{t_1}^{t_2} CApB(t, i) dt$$

where t denotes the MD time of each simulation, with t_1 and t_2 set to be 170 ns and 200 ns, respectively. $i = 1 \sim N$ is the index for the adsorbed situation of each sequence, with N (the number of the adsorbed situation. Namely, at the simulation time $t = 200$ ns, $CApB > 0.1 \text{ nm}^2$).

Table S1. Oligonucleotide sequences used in this study.

Name	Sequence (5'-3')
A ₇	FAM-AAAAAAAA
A ₃ T ₁ A ₃	FAM-AAATAAA
A ₃ T ₂ A ₃	FAM-AAATATAA
A ₃ T ₃ A ₃	FAM-AAATTTAAA
A ₃ T ₄ A ₃	FAM-AAATTTTAAA
A ₃ T ₅ A ₃	FAM-AAATTTTTAAA
(AT) ₅ A	FAM-ATATATATATA
T ₁₁	FAM-TTTTTTTTTTTT
A ₁₀	AAAAA AAAAA TTTTT ATgAT gTTCg TTgTg-FAM
A ₁₅	AAAAA AAAAA AAAAA TTTTT ATgAT gTTCg TTgTg-FAM
A ₂₀	AAAAA AAAAA AAAAA AAAAA TTTTT ATgAT gTTCg TTgTg-FAM
A ₃₀	AAAAA AAAAA AAAAA AAAAA AAAAA AAAAA TTTTT ATgAT gTTCg TTgTg-FAM
A ₄₀	AAAAA AAAAA AAAAA AAAAA AAAAA AAAAA AAAAA AAAAA TTTTT ATgAT gTTCg TTgTg-FAM

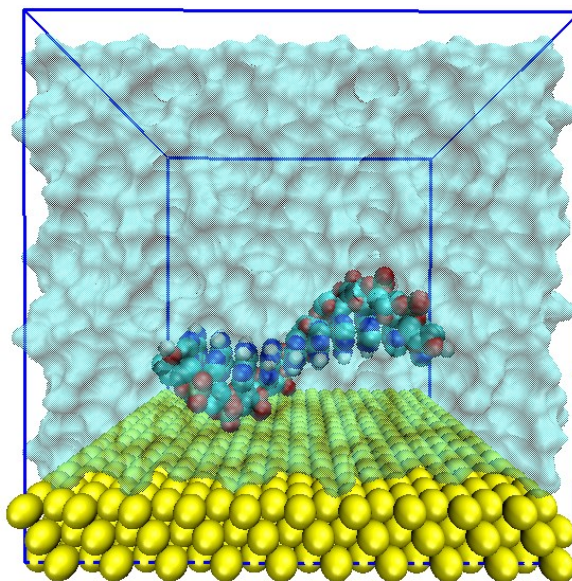


Figure S1. A typical structure at the initial time of the MD simulation. The initial configuration for the hybrid systems is considered by keeping the ssDNA at about 10.0 Å distance away from the gold surface.

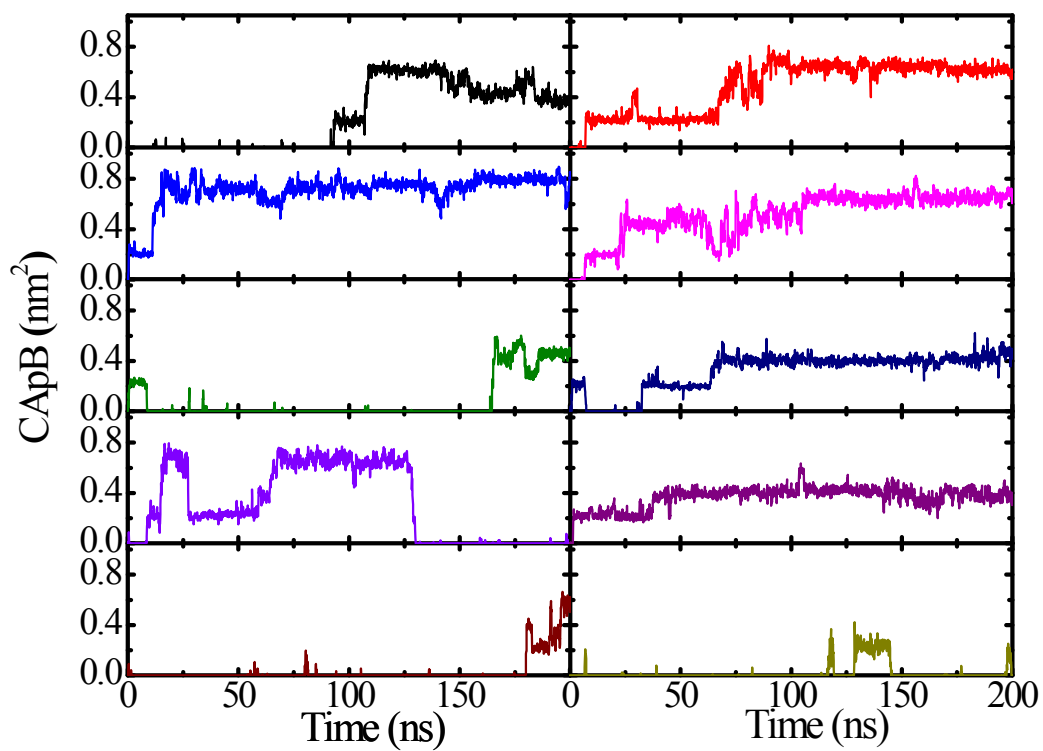


Figure S2. Ten trajectories of the contact area per base (CApB) for the A_7 sequence adsorbing on the gold surface at a temperature $T = 300$ K.

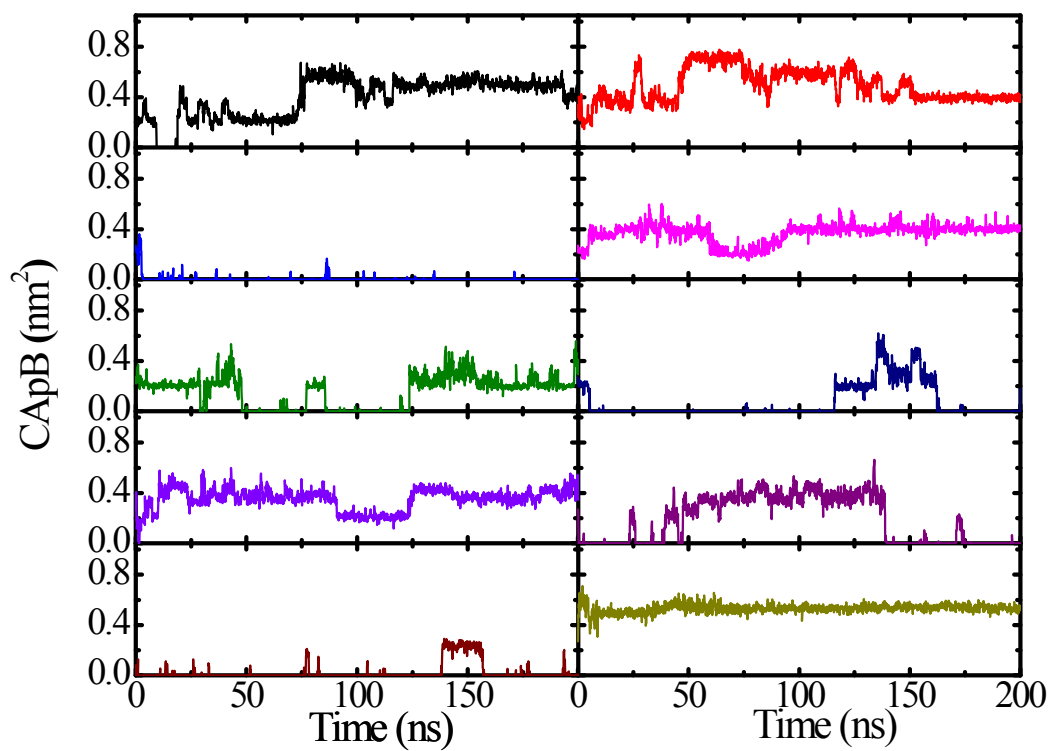


Figure S3. Ten trajectories of CApB for the A_3TA_3 sequence adsorbing on the gold surface at a temperature $T = 300$ K.

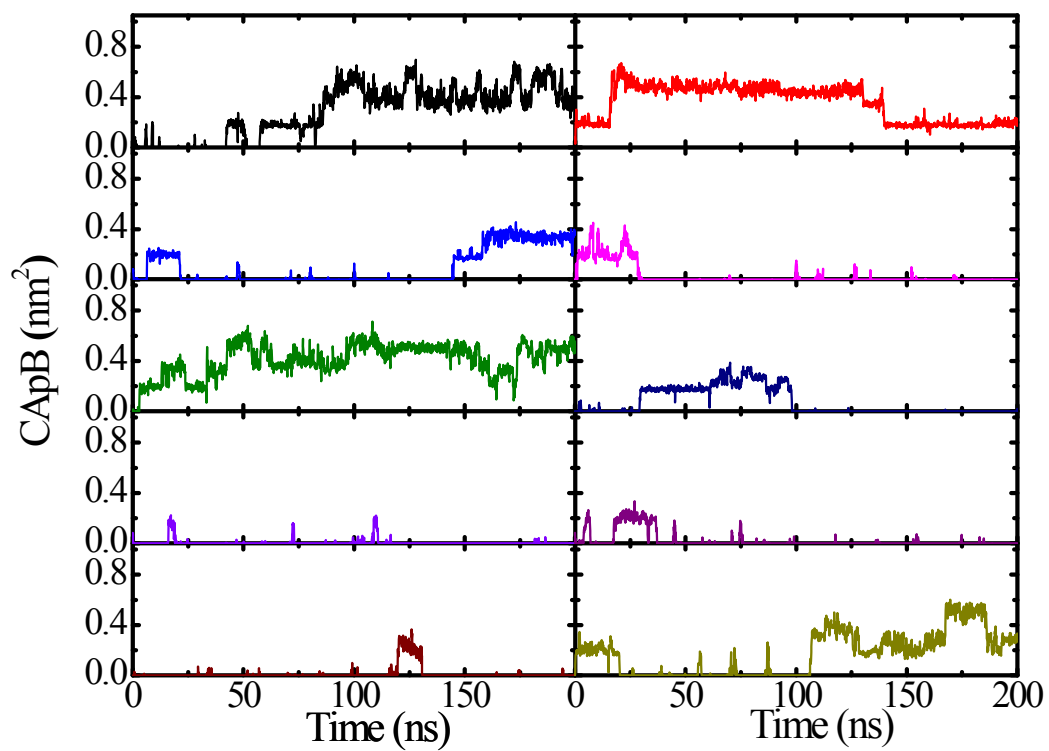


Figure S4. Ten trajectories of C_{ApB} for the A₃T₂A₃ sequence adsorbing on the gold surface at a temperature T = 300 K.

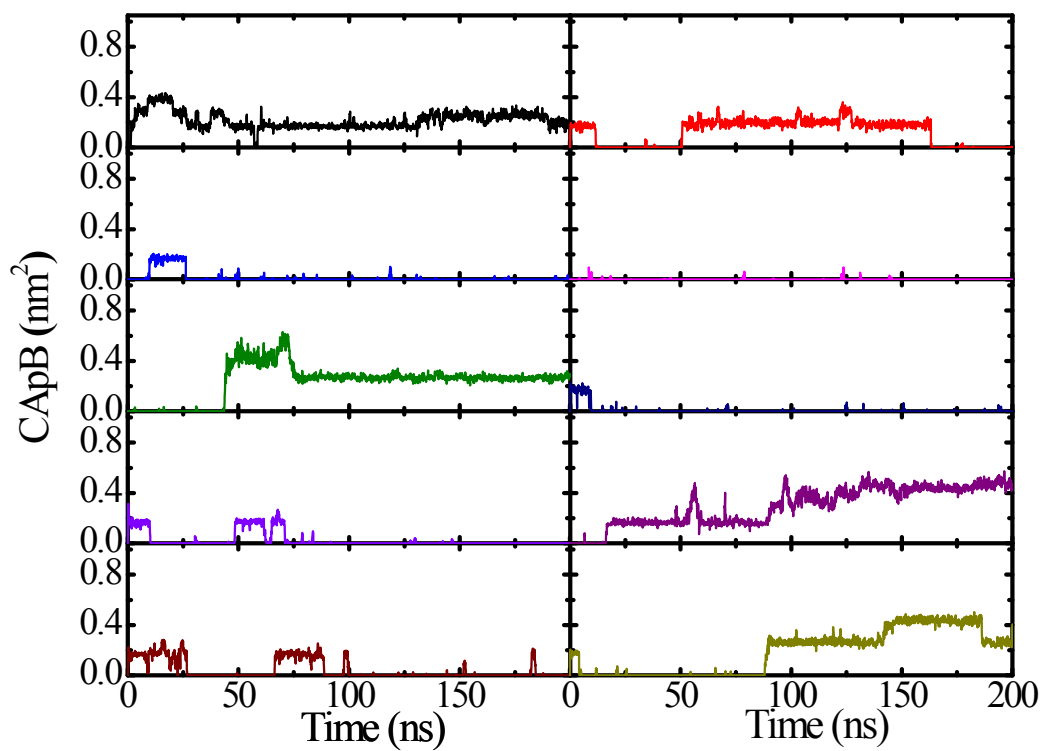


Figure S5. Ten trajectories of CApB for the $A_3T_3A_3$ sequence adsorbing on the gold surface at a temperature $T = 300$ K.

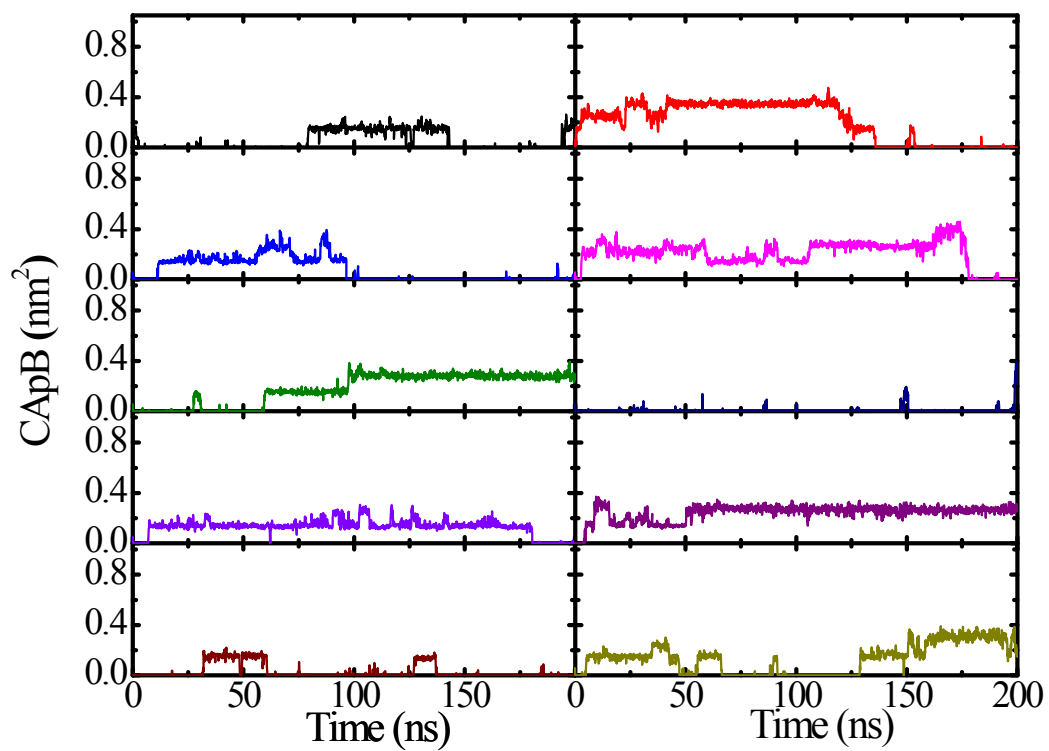


Figure S6. Ten trajectories of CAPB for the $A_3T_4A_3$ sequence adsorbing on the gold surface at a temperature $T = 300$ K.

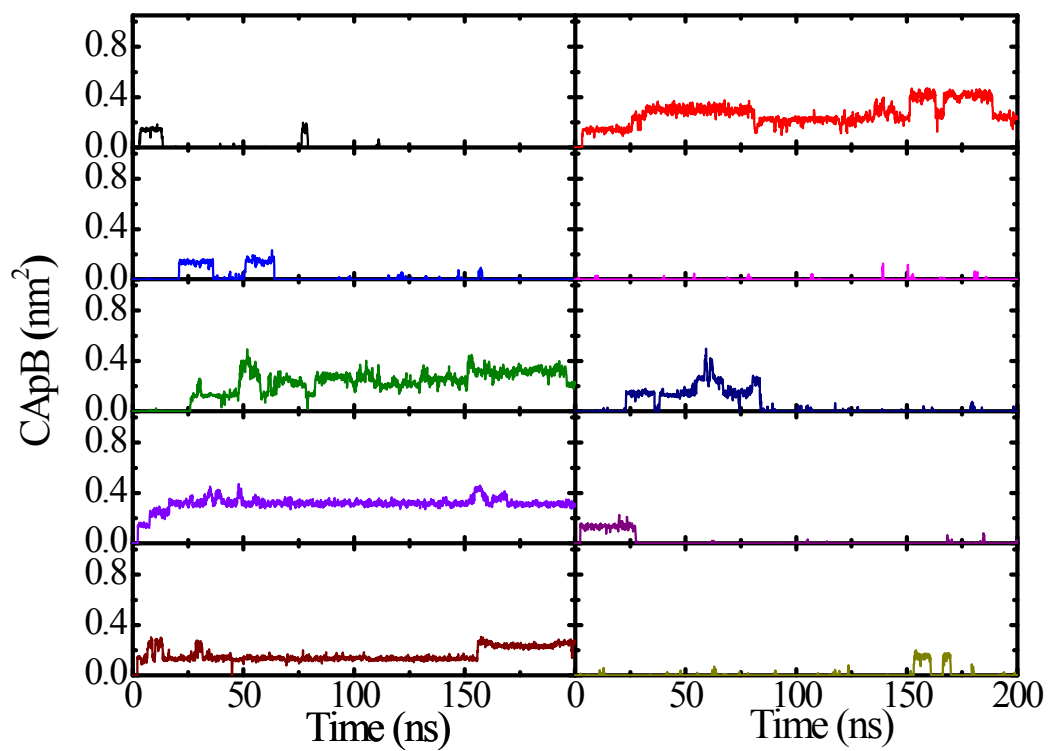


Figure S7. Ten trajectories of CAPB for the $A_3T_5A_3$ sequence adsorbing on the gold surface at a temperature $T = 300$ K.

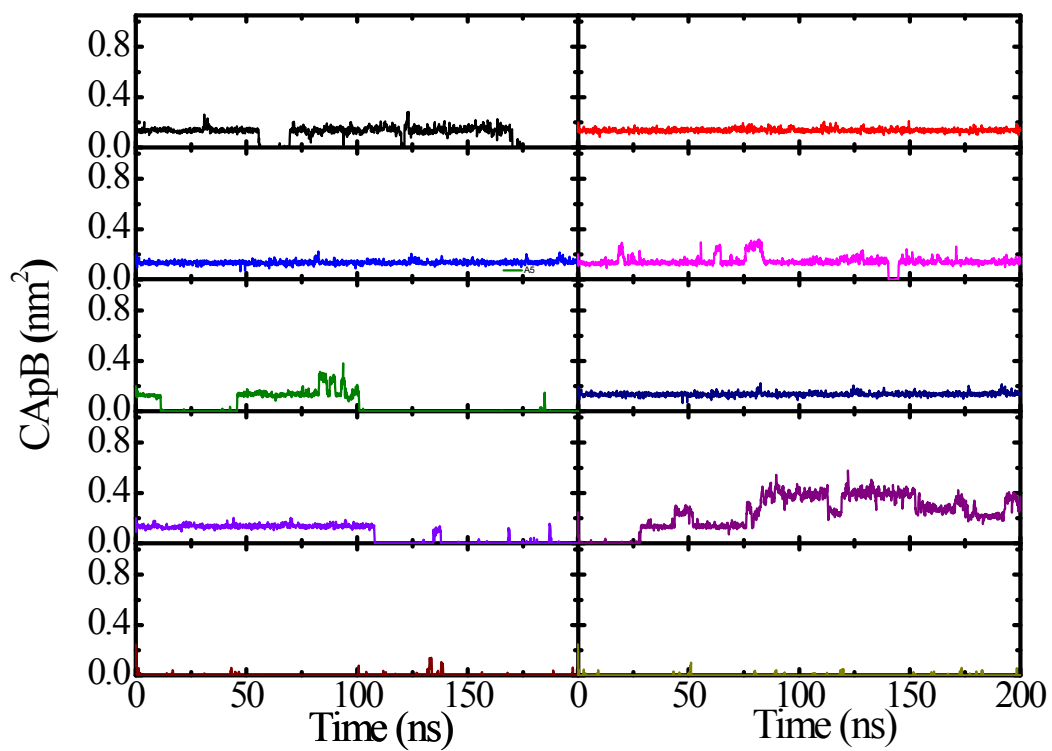


Figure S8. Ten trajectories of CAPB for the (AT)₅A sequence adsorbing on the gold surface at a temperature $T = 300$ K.

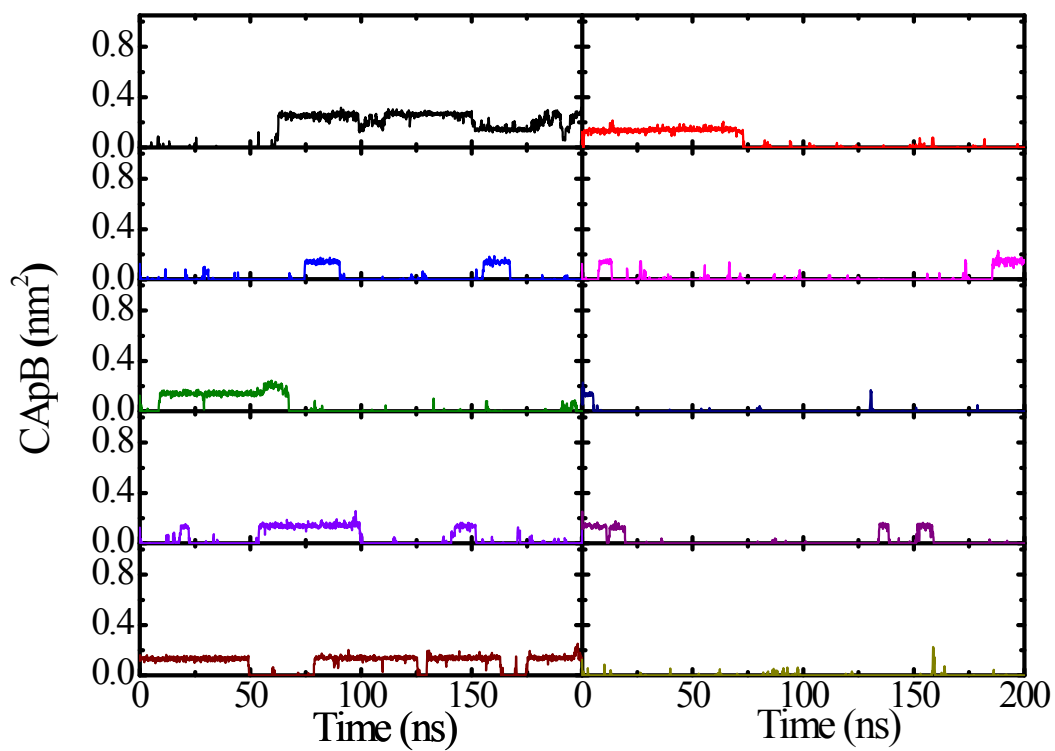


Figure S9. Ten trajectories of CApB for the T_{11} sequence adsorbing on the gold surface at a temperature $T = 300$ K.

Reference

1. E. M. Nelson and L. J. Rothberg, *Langmuir*, 2011, **27**, 1770-1777.
2. X. Zhang, B. W. Liu, N. Dave, M. R. Servos and J. W. Liu, *Langmuir*, 2012, **28**, 17053-17060.
3. S. J. Hurst, A. K. R. Lytton-Jean and C. A. Mirkin, *Anal. Chem.*, 2006, **78**, 8313-8318.
4. X. Jiang, J. Gao, T. Huynh, P. Huai, C. Fan, R. Zhou and B. Song, *J. Chem. Phys.*, 2014, **140**, 234102.